RESEARCH ARTICLE

Macromolecular Reaction Engineering
www.mre-journal.de

Functionalization of Polymer Networks to Target Trans-Resveratrol in Winemaking Residues Supported by Statistical Design of Experiments

Amir Bzainia, Rolando C. S. Dias, and Mário Rui P. F. N. Costa*

The present work aims to produce functionalized polymer networks to target the bioactive molecule trans-resveratrol found in winemaking residues, specifically at grape stems. The synergistic choice of photoinitiation, polymerization composition, and molecular imprinting approach allows the functionalization of these materials. Experimental design is applied to methodically perform the syntheses. The amount of crosslinker, the total monomer's concentration, and the ratio of trans-resveratrol to the functional monomer 4-vinylpyridine (4VP) are the factors selected for this experimental design. The binding capacities and the selectivity of the synthesized materials are assessed through sorption experiments in acetonitrile and hydroalcoholic media. Consequently, a multivariate linear regression analysis leads to describe the uptake of trans-resveratrol by the materials in both media. The crosslinker content and the ratio of trans-resveratrol to 4VP are found to be impactful parameters while designing such materials. These studies allow the identification of working conditions for sorption/desorption processes combining a high retention capability of the adsorbents with selectivity. Furthermore, four materials are selected to enrich trans-resveratrol from grape stems extracts in a continuous process of solid-phase extraction. The results show that the functionalized materials are able to enrich 12-fold the content of trans-resveratrol in some fractions demonstrating the interest of such polymers.

1. Introduction

A major goal of polymer chemistry is the production of functional materials with real-life applications. Such materials can be obtained by carrying out a direct polymerization or a postpolymerization. Although both methods lead to the functionalization of polymeric networks, they are quite different approaches. Direct polymerization is a one-step method in which monomers containing the desired functional groups (e.g., pyridine, boronic acid moieties, aromatic rings) are polymerized. This results in a polymeric network embedding monomer units which confer the desired functionalization to the material.[1] On the other hand, post-polymerization is a two-step approach where a reactive polymeric precursor is synthesized and is next modified through reactive pendent groups. This approach entails more reaction steps than the direct one, and it is most often considered when the direct polymerization cannot achieve the desired functionalization.[2]

To further confer more functionalization to the material, a technique called "molecular imprinting" is used to endow the polymeric network with stereospecificity toward a particular compound referred to as the template.[3] Molecular imprinting begins by a precomplexation step where the template assembles with the functional monomer(s) via intermolecular interactions (e.g., hydrogen bonding, Van der Waals, hydrophobic, and in some cases covalent). At this stage, the template is well positioned relative to the functional monomer(s), forming a stable complex. The addition of the initiator as well as the crosslinker agent is carried out in the next step. As the polymerization is initiated at chosen favorable conditions, the crosslinker is copolymerized with the functional monomers, preserving the spatial arrangements of the template-functional monomer(s). At the end of the polymerization, and after proper removal of the template, a polymer with cavities complementary to the target chemical species is obtained, thus designated as a molecularly imprinted polymer (MIP). Simultaneously, a non-imprinted polymer (NIP) is synthesized following the same steps for the MIP, but only omitting the template from the recipe. The NIP is considered as a "blank" material, as it is chemically similar to the MIP thus permitting a comprehensive evaluation of the molecular imprinting process.

A. Bzainia, R. C. S. Dias
Polytechnic Institute of Bragança
Mountain Research Center (CIMO)
Bragança 5300-253, Portugal
E-mail: rdias@ipb.pt
A. Bzainia, M. R. P. F. N. Costa
LSRE-LCM-Laboratory of Separation and Reaction Engineering—Laboratory of Catalysis and Materials
Faculty of Engineering
Department of Chemical Engineering
University of Porto
Porto 4200-465, Portugal

The ORCID identification number(s) for the author(s) of this article can be found under https://doi.org/10.1002/mren.202200076

DOI: 10.1002/mren.202200076

MIPs and NIPs can be prepared by different methods such as bulk polymerization, suspension polymerization, and precipitation polymerization among others.[4] Naturally, each method has its own merits and limitations, yet in this paper the light is shed on the photoinitiated precipitation polymerization which relies on the free radical polymerization (FRP) mechanism. This approach is chosen due to its easy operation, surfactant-free and high yield.[5,6] During a FRP, an initiator is decomposed into free radicals. This action requires a specific amount of energy that can be brought either by heating the polymerization system or by irradiating it with ultraviolet (UV) light, provided that the initiator absorbs at the appropriate wavelength. Thermally initiated polymerizations often provide a high yield due to the favorable dependency of the different polymerization steps on the temperature (Arrhenius law).[7] However, and in case of MIPs synthesis, heat can drastically weaken the intermolecular interactions between template-functional monomer(s).[8,9] In this perspective, UV irradiation seems advantageous to enhance the molecular recognition of the MIPs in a trade-off with the polymerization extent. As a matter of fact, the technique of photopolymerization has already been used to synthesize methacrylate-based polymers[10] and a gel polymer electrolyte based on polyethylene oxide [11] among other materials.[12]

Thus, joining the techniques of molecular imprinting and photopolymerization, one can theoretically form a tailor-made adsorbent capable to retain a specific compound in a selective manner. In this line of thought, trans-resveratrol appears to be an interesting molecule to valorize through these kinds of functionalized materials. Trans-resveratrol is a phenolic compound belonging to the stilbene family, which occurs in considerable amounts in grapes, and it is no wonder that products derived from this fruit such as wine, are rich sources of this bioactive compound.[13] The interest in trans-resveratrol is due to its inherent antioxidant and anti-inflammatory properties suitable to protect against various diseases, namely cardiovascular, cancer and diabetes.[14,15] Actually, besides wine (see Figure S1 of the Supporting Information), trans-resveratrol has been identified in the different parts of the grape berry (e.g., seeds, skin) and the grapevine (e.g., shoots).[16] Parts like the vine shoots and the stems are discarded away prior to the winemaking process. Nevertheless, research has proven that the discarded stems contain the valuable molecule of trans-resveratrol.[17,18] These findings have been further confirmed by Sun et al. who have quantified trans-resveratrol in Portuguese varieties to be around 145.52 mg kg^{-1} of dry weight.[19]

Given the number of parameters involved in the synthesis of functionalized materials (e.g., solvent, amounts of crosslinker, of functional monomers etc.) to target trans-resveratrol, it is futile to follow the univariate method where only one factor is changed at a time while holding the others constant. This is because such approach would result in a high number of experiments and overlook the possible interactions between the studied variables. To overcome these hindrances, factorial designs combined with multiple regression analysis are powerful tools allowing both an efficient planning of the experiments and the determination of the significance of the predictor variables.[20]

In this study, we explore the feasibility of UV-initiated polymerization to yield functionalized materials with high retention or/and selectivity towards trans-resveratrol. In this context, molecularly imprinted polymers and non-imprinted polymers were systematically synthesized using a factorial design. The resulting materials were tested through batch adsorption experiments in two different media (acetonitrile and hydroalcoholic) allowing the assessment of the binding capacities as well as the selectivity of the materials for trans-resveratrol. Multivariate linear regression was applied to the obtained data, therefore, allowing to understand the impact of the studied variables on the synthesis yield, binding capacity, and selectivity of the materials. Based upon the results of the sorption tests, a group of functionalized materials was selected to treat the different extracts of grape in an attempt to significantly enrich the bioactive agent trans-resveratrol.

2. Experimental Section

2.1. Materials

All chemicals were used as purchased, without further purification. Trans-resveratrol (≥ 98%) was purchased from Cayman (USA). The monomer 4-vinylpyridine (4VP, ≥ 95%) was purchased from Alfa Aesar (USA). The styrene monomer (STY, ≥ 99%) and the crosslinker ethylene glycol dimethacrylate (EGDMA, ≥ 98%) were acquired from Sigma Aldrich (Germany). The polymerization initiator 2,2′-azobis(2-methylpropionitrile) (AIBN, ≥ 98%) was purchased from Sigma Aldrich (Germany). The solvent dimethylformamide (DMF, ≥ 99%) was purchased from Acros Organics (Belgium). Ethanol (EtOH, ≥ 99.8%), methanol (MeOH, ≥ 99.8%), acetonitrile (ACN, ≥ 99.9%), and glacial acetic acid (AcOH, ≥ 99.7%) were all acquired from Fisher Chemical (UK). The water used in the experiments is ultrapure water supplied by the local laboratory.

2.2. Instrumentation

Irradiation was carried out with a custom-made UV-reactor supplied by Paralab (Portugal). The dispositive is equipped with four mercury vapor lamps (Philips Actinic BL TL 8 W/10 1FM/10 × 25CC) with a maximum emission at 350 nm. The interior of the reactor is covered with aluminum to reflect the UV light thus making it evenly distributed inside the reactor. Other features such as a thermocouple, gas tubing (to purge the reaction atmosphere from oxygen) and a mechanical agitator are implemented in this UV reaction system. A control system was implemented using a software designed by the same company (Paralab). In the Supporting Information, a scheme depicting this UV reactor is shown in Figure S2 (Supporting Information).

The HPLC system (KNAUER) consisted of a gradient pump (P6.1 L) equipped with a degasser, an autosampler (6.1 L), a column thermostat (CT2.1) and a diode array detector (6.1 L). ClarityChrom was the software allowing the control of the HPLC system. The chromatographic analysis was performed using an Ascentis C18 (SUPELCO) column with a particle size of 5 µm and dimensions 25 cm × 4.6 mm. A gradient of solvents was used as a mobile phase varying from 100% of water–ACN (9:1) to 100% water–ACN (1:9) for 45 min. The mobile phase water pH was adjusted to 3 using acetic acid. The flow rate of the chromatographic

analyses was 1 mL min^{-1}, and the temperature of the column was set at 45 °C.

2.3. Synthesis of the Functionalized Polymers

Throughout this study, a total of 30 materials were synthesized. Six of these materials were synthesized using thermal polymerization, while the others were UV irradiated. To synthesize the molecularly imprinted polymers (MIPs), trans-resveratrol was first dissolved in the adequate solvent which was a mixture ACN-DMF (85:15) or pure ACN, depending on the synthesis recipe. Then, the monomer 4VP was added to the mixture and left in an ultrasound bath for 15 min to promote the intermolecular interactions between the trans-resveratrol and the 4VP. Afterward, STY was added to the reaction mixture and the same step using the ultrasound bath was repeated. Following this, the crosslinker EGDMA was added. Consequently, the initiator AIBN was added to the reaction mixture which was degassed for five minutes using argon to prevent AIBN cleavage by oxygen. For thermal polymerization, the reaction flask was put in a paraffin bath at a controlled temperature of 60 °C and left to react for 24 h. In case of photoinitiation, the reaction flask was placed inside the UV reactor and left to react for 24 h. For each MIP, a corresponding non-imprinted polymer (NIP) was synthesized following the exact same procedure but without including trans-resveratrol in the polymerization mixture. The obtained polymers were cleaned with MeOH–AcOH (9:1) several times using a dialysis membrane (3.5K MWCO, ThermoFisher Scientific) to remove the unreacted reagents as well as the trans-resveratrol from the MIPs. A step of cleaning with MeOH was also performed to remove the acetic acid and then the materials were left to dry under a vacuum. Notice that 16 of the 30 materials were synthesized using an experimental design considering three factors at two levels (2^3 = 8 pairs of MIP-NIP). A discussion regarding this experimental design is held further below in the manuscript.

2.4. Materials Characterization

2.4.1. Gravimetric Analysis

After drying the materials for several days under vacuum, they were accurately weighed to determine the yields of the polymerizations.

2.4.2. FTIR

Fourier-transform infrared spectroscopy (FTIR) was carried out to analyze the synthesized materials after being dried. The apparatus used was a PerkinElmer Spectrum Two, and the characterization was made in attenuated total reflectance (ATR) mode between 4000 cm^{-1} and 450 cm^{-1}.

2.4.3. Sorption Experiments

The synthesized materials were assessed through batch sorption experiments in pure ACN and EtOH–water (8:2) using trans-resveratrol as analyte. The procedure consisted in weighing 5 mg of the material and adding 750 µL of the trans-resveratrol solution (0.1×10^{-3} M) and then leaving the mixture under shaking (80 RPM) for 24 h and at room temperature. For each tested material, a blank batch experiment (where the liquid phase consisted in the solvent exempt from trans-resveratrol) was also carried out to ensure that the material is not releasing any interfering compounds into the liquid phase. At the end of the 24 h, the concentration of the free resveratrol in the liquid phase was determined by UV spectrophotometry (microplate reader, BioteK – EPOCH2) at 305 nm, which corresponds to the maximum wavelength of trans-resveratrol. The amount of the analyte bound to the material was determined by subtracting the amount of free analyte (C_E) from the initial concentration (C_0). This permitted the determination of the binding capacity (Q) of the material using Equation 1 where the concentrations are expressed in mM, V (mL) is the volume of the liquid phase and m (mg) is the mass of the tested polymer (i.e., 5 mg).

$$Q = \frac{\left(C_0 - C_E\right) V}{m} \quad (1)$$

Furthermore, for each pair of MIP-NIP, it was possible to calculate the imprinting factor (IF) by dividing the binding capacity of the MIP by that of the NIP as shown in Equation 2.

$$IF = Q_{MIP} / Q_{NIP} \quad (2)$$

2.5. Multiple Linear Regression

The yield of the polymerizations, the imprinting factors, and the binding capacities of the 16 materials originating from the experimental design were used to define different linear models. To this goal, R-based open-source software was used. Both main and interaction effects were considered in the regression analysis. Based on these linear models, a group of materials was selected for further application in the treatment of grape stems extracts.

2.6. Application of the Synthesized Materials to Target Trans-Resveratrol in Grape Stems Extracts

2.6.1. Grape Stems Extraction

The grape stems residue was supplied by Caves Campelo winery from the region of Barcelos in Portugal. This residue was ground and used to perform two distinct extractions with two different solvents: pure ACN, and EtOH-W (8:2). The extraction procedure consisted in weighing 30 g of grape stems and then add 300 mL of the solvent. The extraction mixture was then left 20 min in an ultrasound bath and in the dark (aluminum foil was used to cover the beaker). Following this, the extraction mixture was left 1 h under magnetic stirring (also in the dark). At the end, the mixture was filtrated in vacuum, resulting in a limpid liquid exempt from solid particles. A difference in color between the two extracts is visible, implying also a dissimilarity in the compositions.

2.6.2. Trans-Resveratrol Identification and Quantification

To identify trans-resveratrol, a standard solution of this analyte was injected in the HPLC and then compared to the chromatograms of both extracts. Furthermore, to permit the quantification of trans-resveratrol, a calibration curve was created. For this, a stock solution of trans-resveratrol was prepared in pure ethanol and then dilutions were made in EtOH–W (8:2) to obtain a series of trans-resveratrol concentrations with values of 2, 10, 50, 100, 250, and 500 mg L^{-1}. Each concentration was then injected in the HPLC allowing the obtention of the correspondent peak area. The calibration curve was then constructed by plotting the peak areas against the analyte concentrations. The method of least squares was used to determine the correlation coefficient as well as the calibration linear equation. This procedure was repeated twice to ensure the accuracy of the calibration equation.

2.6.3. Solid-Phase Extraction Experiments with Grape Stems Extracts

The treatment of both ACN and EtOH–water (8:2) extracts was carried out in solid-phase extraction (SPE) apparatus. The selected functionalized materials were packed (40 mg) into SPE cartridges. Prior to performing the SPE test, the cleanness of the materials was checked using UV spectroscopy and, in some cases, HPLC was used to ensure that no compounds are eluting from the materials. The SPE test consisted in four steps, which are the conditioning of the packed materials, the loading of the extract, the washing of the materials and finally the elution. The solvent of conditioning as well as the washing was the same as one of the extractions (ACN or EtOH–W). In the case of the ACN extract, two successive elution steps were carried out using EtOH–water (8:2) and then MeOH–AcOH (8:2). In the case of the EtOH–W extract, only one elution step was made using MeOH–AcOH (8:2). The obtained fractions of the loadings, washings and eluted fluids were injected into the HPLC. By means of the calibration curve, it was possible to directly quantify the concentration of trans-resveratrol obtained in each fraction of the SPE procedure. This allowed to further calculate the enrichment factors of trans-resveratrol in each fraction. The enrichment factor was calculated by dividing the peak area of trans-resveratrol by the total chromatogram's area. These chromatograms show the absorption at a wavelength of 280 nm.

3. Results and Discussion

3.1. Rationale for Materials Synthesis

Along the manuscript, some key parameters related to the composition of the synthesized polymers are often going to be mentioned. To avoid ambiguities, these parameters are summarized in **Table 1**.

As stated earlier in this paper, the objective of this work is the synthesis of materials with high binding capacity and/or selectivity towards trans-resveratrol. However, this task is not straightforward as various parameters impact the polymerization process and hence the final product. **Table 2** summarizes these parameters and discusses the benefits of using their low or high ranges.

Table 1. Describing parameters of the polymerization runs.

Parameter	Definition
Y_M [%]	Mass fraction of the polymerizable monomers mixture (including functional monomer(s) and crosslinker(s)) in the polymerization solution.
Y_{CL} [%]	Mole fraction of the crosslinker in the polymerizable monomer's mixture.
$Y_{T/FM}$	Mole ratio between the template and a functional monomer.
Y_I (%)	Mole ratio between the initiator and the polymerizable monomers.

3.2. Factorial Design

3.2.1. Preliminary Study

During the process of MIP synthesis, the antioxidant effect of trans-resveratrol, or any polyphenol in general, could drastically decrease the rate of polymerization and even inhibit it through radical cleavage. Additionally, trans-resveratrol is an expensive reagent, so it is advised to proceed carefully before starting a campaign of syntheses. Thus, the first task was to conduct a polymerization through thermal initiation to evaluate the possibility of the use of trans-resveratrol as a template. Thermal initiation was chosen because it was proved to be effective for other templates such as quercetin,[21] gallic acid, and polydatin.[22] Realizing that thermal initiation is possible when trans-resveratrol is present in the polymerization mixture, the next step was to synthesize two materials (a pair of MIP and NIP) using UV irradiation (at room temperature) to assess the inhibitory effect of trans-resveratrol on the polymerization process. **Table 3** reviews the materials synthesized in the framework of this preliminary study. As explained in Table 2, it is preferable to use pure ACN as it interferes the least with the assembly of the template-functional monomer(s). However, dissolving trans-resveratrol in pure ACN and at the same time keeping the parameters of the polymerizations (e.g., Y_{CL}, Y_M etc.) intact is not possible due to the insolubility of trans-resveratrol.[23] Thus, a mixture of ACN–DMF (85:15) was used instead. Sorption experiments using these preliminary materials allowed the determination of their binding capacities and the imprinting factors in acetonitrile (shown in Table 3). Considering Y_M, Y_{CL}, $Y_{Res/4VP}$, $Y_{Res/STY}$ and the initiation mechanism (UV irradiation or at 60 °C) as factors, multiple regression analysis was carried out to analyze the variation of the binding capacity. Considering only the main effects, the linear model gave an adjusted R^2 of 0.9317, ($p = 0.00282 < 0.05$) with Y_{CL} being the only significant predictor (p-value $= 0.0152 < 0.05$). This means that the amount of crosslinker directly impacts the binding capacity of the materials and thus it should be considered in the further experimental design. Moreover, the materials M2, N2, M3, N3, M4, and N4 have an Y_M between 12% of 5% which resulted in a small particle size. This has serious repercussions on the usability of such materials in continuous processes such as SPE or frontal analysis, as loss of material would be inevitable.

Additionally, the preliminary results show that a high amount of crosslinker (e.g., 82.4% for M1 and N1) leads to a low binding capacity but a relatively high imprinting factor. On the other hand, decreasing the amount of crosslinker appears to promote

Table 2. Potential effect of the polymerization conditions on the functionalization of polymer networks.

Parameter	High range	Low range
Crosslinker content (Y_{CL})	Geometrical stability of binding sites. High mechanical resistance (e.g., $Y_{CL} > 80\%$).	Enhancement of the functional groups density and increase of interaction possibilities (e.g., $Y_{CL} < 50\%$).
Composition of the functional monomers' mixture	Exploiting multiple interactions between complex templates and different functional monomers (e.g., 4VP + styrene for hydrogen bonding and π–π stacking).	Simplicity of polymerization recipe, avoiding heterogeneity of polymer networks due to different incorporation rates for the diverse functional monomers (e.g., single functional monomer).
Total monomers' concentration (Y_M)	Good polymer yield; fast polymerization (e.g., $Y_M > 25\%$).	Control of particle size and morphology with enhancement of mass transfer; control of reaction temperature; solubilization of initial reactants (e.g., $Y_M < 10\%$).
Template content ($Y_{T/FM}$)	Increasing stereospecific cavities for molecular recognition (e.g., $Y_{T/FM} > 1/3$).	Increase the functional groups of the material while decreasing its specificity (lesser stereospecific cavities). Avoiding solubility problems, polymerization inhibition, material cleaning difficulties and high price caused by template inclusion (e.g., $Y_{T/FM} = 0$ for NIPs).
Solvent hydrogen bonding capacity and polarity	Good solubility of monomers and templates (e.g., inclusion of DMF or DMSO).	Decreasing competition with template/functional monomers self-assembly Higher control on polymer particles morphology and size through phase separation (e.g., 100% ACN).
Polymerization temperature and initiation mechanism	High polymer yield and diverse initiation possibilities (e.g., $T > 60$ °C with thermal initiators).	Improve the template/functional monomers self-assembly (e.g., $T <$ 30 °C with photopolymerization).

Table 3. Preliminary synthesized materials and their respective binding capacities and imprinting factors (sorption tests were carried out in acetonitrile, $n = 4$).

Material	Y_M	Y_{CL}	$Y_{Res/4VP}$	$Y_{Res/STY}$	Y_I	Yield	Initiation mechanism	Qads (mean ± SD, μmol g^{-1})	IF (mean ± SD)
M1	21.40	82.4	1/2	1/1	5.36	99.61	Thermal (60 °C)	1.55 ± 0.05	2.57 ± 0.49
N1			0/2	0/1		96.88		0.68 ± 0.13	
M2	5.78	40	1/2	1/1	5.2	83.68	Thermal (60 °C)	10.15 ± 0.25	0.82 ± 0.03
N2			0/2	0/1		91.92		12.45± 0.23	
M3	12.74	42.42	1/5	1/2	5.35	92.88	Thermal (60 °C)	11.32 ± 0.13	0.99 ± 0.04
N3			0/5	0/2		99.27		11.10±0.35	
M4	12.74	42.42	1/5	1/2	5.3	55.74	UV irradiation	12.78 ± 0.96	1.25±0.05
N4			0/5	0/2		89.23		10.19 ± 0.70	

the retention of trans-resveratrol but at the cost of the material selectivity.

Regarding the initiation mechanism, a simple comparison between the pairs M3-N3 and M4-N4 shows that a higher IF is obtained when UV irradiation is used to initiate the polymerization. This outcome is interesting since it shows that performing the polymerization at room temperature (photoinitiation) preserves the trans-resveratrol-functional monomer(s) interactions better than the thermal initiation at 60 °C. As a matter of fact, this outcome was confirmed by Navarro-Villoslada et al., who have demonstrated that materials synthesized at room temperature have higher affinity than the ones synthesized at high temperature.[24]

3.2.2. Choice of Factors and Type of the Factorial Design

The objective of this study is to optimize the binding capacity or/and the selectivity of the synthesized polymers towards resveratrol. For this end, three factors were deemed essential to optimize, which are: Y_M, Y_{CL} and $Y_{Res/4VP}$. A two-level factorial design (2^3) was chosen resulting in 16 materials (eight pairs of MIP-NIP). The levels chosen for each factor are shown in **Table 4**. The cube plot of the chosen factorial design is shown in Figure S3 (Supporting Information).

Table 4. Impactful factors and their respective levels.

Parameter	Low level	High level
Y_M	20%	30%
Y_{CL}	40%	60%
$Y_{Res/4VP}$	1/7	1/3

The choice of 4-vinylpyridine (4VP) as a functional monomer stems from previous works as well as recent publications regarding this matter. In fact, in a recent work by Cao et al., different types of functional monomers (methacrylic acid, acrylamide, 2-vinylpyridine and 4-vinylpyridine) were used to synthesize MIPs

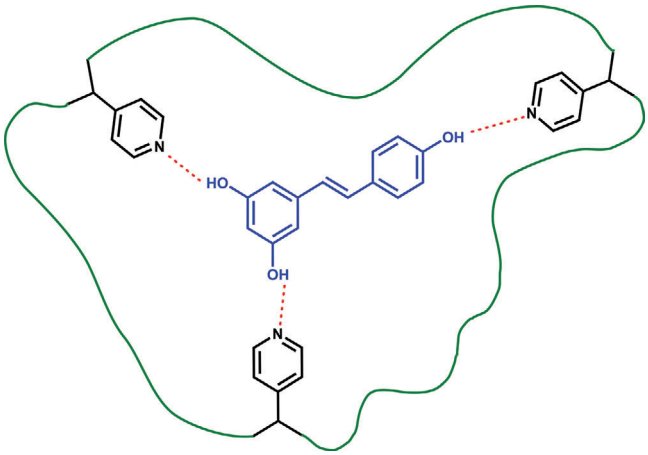

Figure 1. Depiction of the molecular interactions between trans-resveratrol (in blue) and 4VP monomer units (in black). The hydrogen bonds are illustrated by dotted red lines. The green line is a generic representation of the polymer chains.

to target trans-resveratrol. Their results showed that when 4VP is selected as the functional monomer, the binding capacity and the selectivity of the material were the highest.[25] This is due to the hydrogen bonds established between the 4VP monomer units and the hydroxyl moieties of trans-resveratrol, as shown in **Figure 1**. Other works demonstrate the efficacy of 4VP as a functional monomer to target polyphenols.[26–28] $Y_{Res/4VP}$ was varied between 1/3 and 1/7. The former level is based on thermodynamic data that demonstrate that the assembly of 4VP with trans-resveratrol is the most stable at a ratio of 3 to 1.[29] The latter level was chosen to evaluate the possibility of the generation of selective material even when employing a low amount of template during the synthesis. Based on the preliminary studies, a value of Y_M = 12% cannot be used since it will result in a material with low particle size, limiting its potential use in the treatment of grape stems extract. Concerning the amount of crosslinker, values between 40% and 60% were chosen, which seemed to be the sweet spot to obtain materials with a reasonable binding capacity without sacrificing the selectivity. **Table 5** resumes the polymerization runs dictated by the chosen experimental design.

Besides the 16 materials dictated by the factorial design, six others were synthesized using the univariate approach to assess the influence of the styrene incorporation and the synthesis solvent on the final materials. M5_Bis and N5_Bis were both synthesized in a similar way as M5 and N5 but without the inclusion of styrene in the synthesis recipe. On the other hand, to assess the effect of the synthesis solvent, M13 and N13 were synthesized in pure ACN and M13_Bis and N13_Bis were synthesized using ACN-DMF (85:15) as solvent. **Table 6** describes the synthesis conditions of these additional materials.

4. Characterization of the Synthesized Materials

In order to determine the final composition of the synthesized materials, and whether the utilized monomers were incorporated in the polymeric network, FTIR analysis was carried out for each material. Since the number of materials is relatively high (22 materials including the additional ones), we chose to include in the main manuscript some representative examples in which the main functional groups are existent. The other FTIR spectra were included in Figures S4 and S5 (Supporting Information).

From **Figure 2**, it is apparent that the FTIR spectra of both N5 and M5 (c and d) present a peak at 702 cm^{-1} which is characteristic of the aromatic benzene ring. This peak is not present in the FTIR spectra of N5_Bis and M5_Bis (a and b). This result confirms the styrene incorporation into the materials since the difference between M5-N5 and M5_Bis-N5_Bis is the presence of the styrene monomer in the initial polymerization mixture. Regarding the 4VP monomer, characteristic peaks at 1600 cm^{-1} (C=C pyridyl), 1418 cm^{-1} (C=N), 820 cm^{-1} and 755 cm^{-1} (both correspond to the C–H bending in the pyridine ring) are all indicators of the successful polymerization of this monomer and its existence in the synthesized materials. The last monomer unit that should be present in the synthesized materials is the crosslinker EGDMA. Characteristic peaks of this latter appear at 1720 cm^{-1} and 1130 cm^{-1} which are assigned to the functional groups of C=O and C–O respectively, confirming the polymerization of the crosslinker.

Table 5. Syntheses resulting from the 2^3 factorial design (the initiation was carried out through UV irradiation).

Material	Y_M	Y_{CL}	$Y_{Res/4VP}$	$Y_{Res/STY}$	Y_I	Yield	Solvent
M5	20	40	1/3	1/1	5.2	35.64	ACN–DMF (85:15)
N5			0/3	0/1		97.93	
M6	30	40	1/3	1/1	5.2	39.56	ACN–DMF (85:15)
N6			0/3	0/1		102.46	
M7	20	60	1/3	1/1	5.2	60.23	ACN–DMF (85:15)
N7			0/3	0/1		101.54	
M8	30	60	1/3	1/1	5.2	66.96	ACN–DMF (85:15)
N8			0/3	0/1		102.85	
M9	20	40	1/7	1/1	5.2	44.23	ACN–DMF (85:15)
N9			0/7	0/1		101.29	
M10	30	40	1/7	1/1	5.2	36.37	ACN–DMF (85:15)
N10			0/7	0/1		109.90	
M11	20	60	1/7	1/1	5.2	72.45	ACN–DMF (85:15)
N11			0/7	0/1		103.55	
M12	30	60	1/7	1/1	5.2	74.95	ACN–DMF (85:15)
N12			0/7	0/1		104.31	

Table 6. Polymerization conditions of the additional materials using the univariate approach (initiation was carried out through UV irradiation).

Material	Y_M	Y_{CL}	$Y_{Res/4VP}$	$Y_{Res/STY}$	Y_I	Yield	Solvent
M5_Bis	20	40	1/3	1/0	5.2	24.77	ACN–DMF (85:15)
N5_Bis			0/3	0/0		102.80	
M13	14.4	75	1/3	1/1	5.2	71.13	Pure ACN
N13			0/3	0/1		100.55	
M13_Bis	14.4	75	1/3	1/1	5.2	84.87	ACN–DMF (85:15)
N13_Bis			0/3	0/1		106.52	

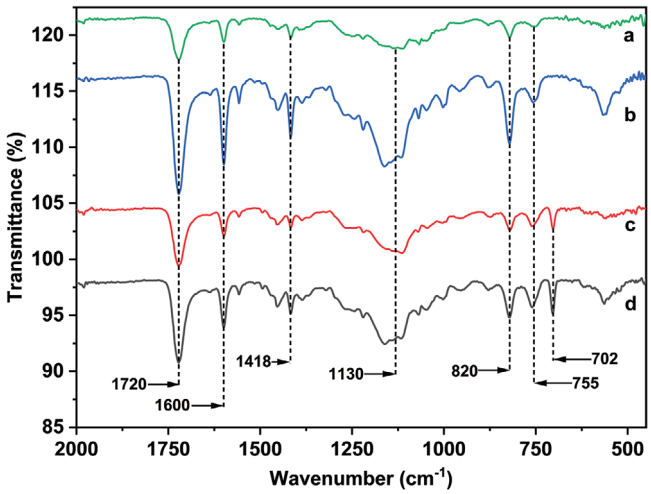

Figure 2. Representative FTIR spectra of synthesized materials. a) N5_Bis; b) M5_Bis; c) N5; d) M5.

4.1. Impact of the Synthesis Recipe on the Polymerization Yield

In Table 5, the yield of each polymerization is shown. To make use of such data, multiple linear regression analysis was conducted. Y_{CL}, Y_M, and $Y_{Res/4VP}$ were the variables used to construct the linear model with the yield being the response variable. Three linear models were attempted considering the interactions between the factors. The obtained results are shown in Table S1 (Supporting Information). The linear model which considers only the main effects had the highest adjusted R^2, highest F-statistic and a p-value that is much lower than the threshold of 0.05. Equation 3 describes the linear variation of the yield in the function of Y_{CL}, Y_M, and $Y_{Res/4VP}$. Based on this model, contour plots of the combined effects of both Y_{CL}, $Y_{Res/4VP}$ and Y_M, $Y_{Res/4VP}$ were created and are shown in **Figure 3**.

$$\text{Yield} = 54.25 + 0.26\ Y_M + 0.75\ Y_{Cl} - 164.63\ Y_{Res/4VP} \quad (3)$$

These results demonstrate that the main factor that contributes to the variation of the yield, is the amount of trans-resveratrol in the polymerization system expressed by the parameter $Y_{Res/4VP}$ ($p < 0.001$). The less trans-resveratrol, better is the yield, which is logical since trans-resveratrol is an antioxidant molecule capable of cleaving free radicals responsible for the initiation and the propagation of the polymerization. One can argue that it is possible to use an equivalent amount of initiator to compensate the antioxidant effect of the template, however this approach would lead to different average molecular weight between the MIP and the NIP which lead to incomparable materials. Regarding the other parameters of Y_{CL} and Y_M, their coefficients are low (and p values higher than 0.05) meaning that they don't impact the yield as the quantity of trans-resveratrol does.

Interestingly, the material M5_Bis, which was synthesized without the inclusion of styrene, had a very low polymerization yield (≈25%) suggesting that the monomer of styrene plays a role in the propagation of the polymerization acting like another source of free radicals. Therefore, the final mass of M5_Bis was about 24 mg which was not sufficient to use in the treatment of the grape stems extracts.

4.2. Sorption Experiments

In this section, the results of the static sorption tests are presented in both acetonitrile and hydroalcoholic solution. The results consist in the binding capacity and the imprinting factor of each synthesized material. Furthermore, multiple linear regression analysis was carried out to determine the effect of the synthesis conditions on the binding capacities and the imprinting factors. A special focus was attributed to the results of acetonitrile due to the low interference of this solvent in the process of trans-resveratrol binding to the materials. It is important to emphasize that the regression analysis only considered the materials stemming from the factorial design.

4.2.1. Acetonitrile as a Testing Medium

Figures 4 and **5** summarize respectively the results of the binding capacities and the imprinting factors of the synthesized materials (the numerical data can be consulted in Table S2, Supporting Information). The results of the binding capacities and the imprinting factors of M5, N5 and M5_Bis and N5_Bis, show no significant difference. This implies that the incorporation of styrene in the polymerization mixture has almost no effect on the material's functionality. However, the decision of the inclusion of the styrene into the synthesis recipes was linked to the final objective of this work which is the application of the functionalized materials in the enrichment of trans-resveratrol from hydroalcoholic solutions. In this context, the use of styrene would confer more hydrophobicity to the materials which would increase the affinity with the target compound in a polar protic solvent.

Comparing the materials made in pure acetonitrile (M13 and N13) with the ones made in the ACN–DMF mixture (M13_Bis and N13_Bis) one can notice the gap between the imprinting factor of the pair M13-N13 and the pair M13_Bis-N13_Bis. Such result shows the interest of use of synthesis solvents that have low interference with the trans-resveratrol-4VP hydrogen bonding. Since ACN is much less protic than DMF, it would strengthen the affinity between the trans-resveratrol and the functional monomer of 4VP in the polymerization mixture, which would result in more stereospecific cavities dedicated to the trans-resveratrol compound. As a consequence, M13 had a superior binding capacity compared to M13_Bis.

Regarding the other materials, the multiple linear regression tool was used, thus yielding the empirical relations describing the binding capacity (Q) and the imprinting factor (IF) as shown in **Table 7**. Other linear models considering the two-way and three-way interactions were also calculated and the results were put in Tables S3 and S4 of Supporting Information. Furthermore, contour plots of the effect of Y_{CL}, Y_M and $Y_{Re/4VP}$ on both Q and IF are shown in **Figure 6**.

Both the linear regression equation and the contour plots show a clear dependency of the binding capacity (Q) on the crosslinker content (Y_{CL}) and the trans-resveratrol content ($Y_{Res/4VP}$). In fact, as Y_{CL} diminishes, the polymer chains contain more 4VP

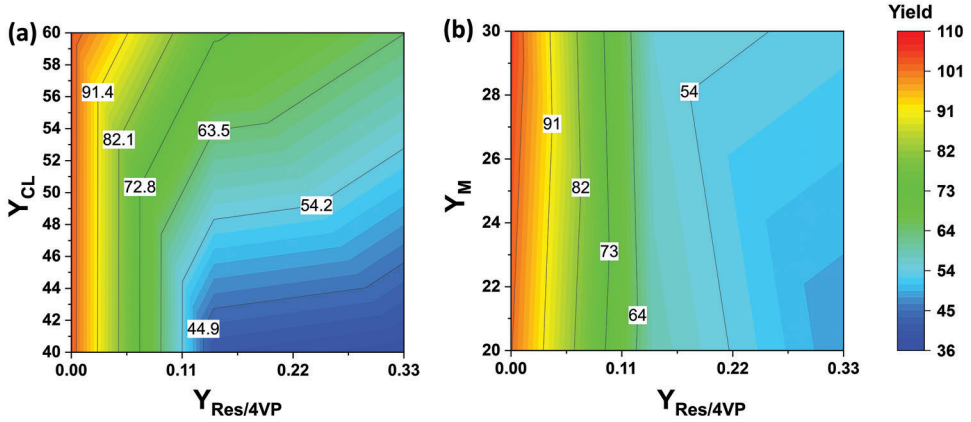

Figure 3. Contour plots of the combined effects of the crosslinker content, total monomer concentration and resveratrol content on the polymerization yield. a) Contour plot of the combined effects of the crosslinker content (Y_{CL}) and the trans-resveratrol content ($Y_{Res/4VP}$); b) Contour plot of the combined effects of the total monomer concentration (Y_M) and the resveratrol content ($Y_{Res/4VP}$).

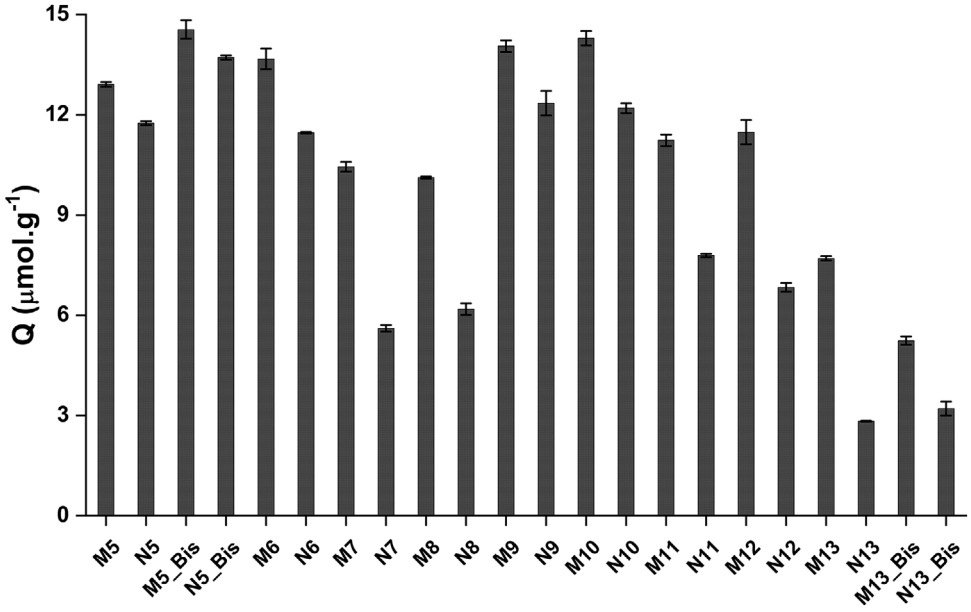

Figure 4. Binding capacity of the synthesized materials using 0.1×10^{-3} M trans-resveratrol in ACN and at room temperature ($n = 2$).

monomer units which are responsible for the binding of trans-resveratrol to the material. Additionally, the data demonstrates that the trans-resveratrol-imprinted materials ($Y_{Res/4VP} > 0$) have higher binding capacity than the non-imprinted materials. Moreover, the model as well as the 2D contour plot show no significant variation of the binding capacity with Y_M, suggesting that the total monomer concentration (which eventually affects the size of the polymer particles) does not affect the adsorptive capacity of the materials. Such result is expected, since a batch sorption experiment lasts for 24 h allowing the system to reach the equilibrium. At these conditions, having high or low particles size would not affect the diffusion of trans-resveratrol through the material.

Table 7. Linear models describing the binding capacity (Q) and the imprinting factor (IF) of the materials tested in pure ACN.

Response variable	Model equation	Adjusted R^2	p-value of the model	Significant parameter(s)
Q	$Q = 20.0590 + 0.0014\ Y_M - 0.2062\ Y_{CL} + 8.3111\ Y_{Res/4VP}$	0.7105	0.000405	Y_{CL}: $p < 0.001$ $Y_{Res/4VP}$: $p < 0.05$
IF	$IF = -0.0587 + 0.0034\ Y_M + 0.0253\ Y_{CL} + 0.4746\ Y_{Res/4VP}$	0.7806	0.0282	Y_{CL}: $p < 0.01$

Table 8. Linear model of the binding capacity (Q) and the imprinting factor (IF) of the materials tested in EtOH–water (8:2).

Response variable	Model equation	Adjusted R^2	p-value of the model	Significant parameter(s)
Q	$Q = 10.4222 - 0.0715\ Y_M - 0.1024\ Y_{Cl} - 4.6479\ Y_{Res/4VP}$	0.6447	0.001346	Y_{CL}: $p < 0.001$ $Y_{Res/4VP}$: $p < 0.05$
IF	$Q = 10.4222 - 0.0715\ Y_M - 0.1024\ Y_{Cl} - 4.6479\ Y_{Res/4VP}$	0.543	0.1161	Y_{CL}: $p < 0.1$

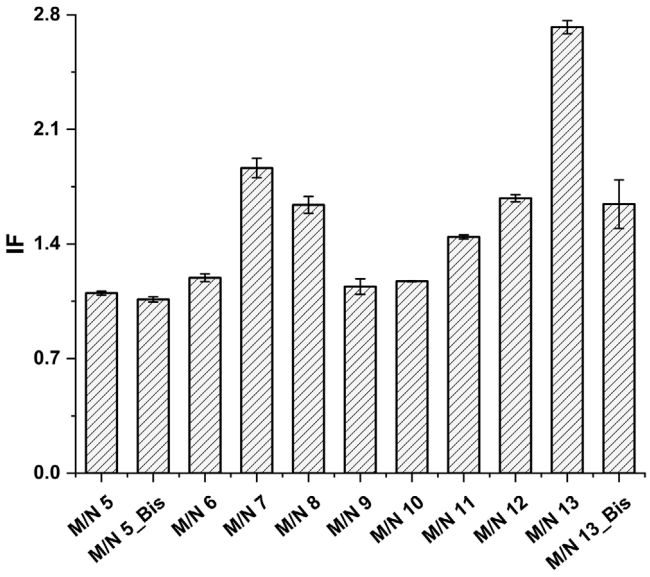

Figure 5. Imprinting factor (IF) of the synthesized materials using 0.1×10^{-3} M trans-resveratrol in ACN and at room temperature ($n = 2$).

However, this outcome may change if the materials are tested in a continuous sorption experiment (lower particle size promotes the diffusivity of the analytes).

In relation to the imprinting factor (IF), a significant positive dependency on Y_{CL} was found ($p < 0.01$). This indicates that increasing the amount of the crosslinker while having trans-resveratrol in the polymerization mixture, improves the process of formation of the specific cavities which would eventually yield materials capable of recognizing trans-resveratrol. Apart from that, the IF does not appear to depend on the parameter Y_M, although the parameter $Y_{Res/4VP}$ seems to influence the molecular recognition of the materials. In fact, an $Y_{Res/4VP} = 1/3$ (M7 and M8) leads to a higher IFs than an $Y_{Res/4VP} = 1/7$ (M11 and M12).

4.2.2. Hydroalcoholic Mixture as a Testing Medium

It was expected that the results obtained in a hydroalcoholic medium would be drastically different from the ones obtained in pure acetonitrile. This is because the ethanol–water mixture interferes with the hydrogen bonds susceptible to occur between the pyridyl functions of the material (due to the 4VP monomer) and trans-resveratrol (through the hydroxyl functions). **Figures 7** and **8** show the results related to the binding capacities of the materials and their imprinting factors (the numerical data can be consulted in Table S5, Supporting Information). In line with the hypothesis stated above, the overall adsorptive capacity of the synthesized materials decreased significantly and almost all of them lost their molecular recognition in the hydroalcoholic mixture (IFs below or barely equal to one). To further understand the behavior of the synthesized materials in a polar protic medium, multiple linear regression models were estimated and listed in **Table 8** (considering materials stemming from the factorial design). Other linear models were attempted, and their output was placed in Tables S6 and S7 (Supporting Information). The parameter $Y_{Res/4VP}$ has a negative correlation with the binding capacity of the materials, implying that having more imprinted cavities (due to the higher amount of trans-resveratrol in the initial polymerization mixture) does not enhance the binding capacity in this ethanol–water mixture. The same goes for the parameter Y_{CL}, since increasing the quantity of crosslinker would automatically lower the monomer units of 4VP in the polymer chains, resulting in a less functionalization of the materials. Concerning the IF linear equation, its p-value is higher than the benchmark value of 0.05. Thus, it is not recommended to further utilize this model due to hidden factors related to the nature of the medium that is not accounted for.

Now comparing the materials M5, N5 with M5_Bis, N5_Bis (exempt from styrene), the material performance does not seem to substantially change when styrene is added to the polymerization recipe. However, it is likely that using different ratios $Y_{Res/STY}$ would impact the final characteristics of the material. Another relevant comparison is the one between M13 (synthesized in pure ACN) and M13_Bis. Despite the performance gap that the M13 demonstrates in pure acetonitrile compared to M13_Bis, both materials behave in a similar manner in the EtOH–water mixture. This confirms again that targeting trans-resveratrol in such a medium is challenging due to the interference of the solvent in the intermolecular interactions.

5. Enrichment of Trans-Resveratrol from Grape Stems Extracts

5.1. Criteria for Materials Selection

Since the aim of this work is to enrich trans-resveratrol from grape stems extracts, choosing materials with high imprinting factors should help achieve this goal. In addition to this parameter, choosing materials with relatively high binding capacity is of equal importance. We also hint that the criteria of selection were based on the results obtained in pure ACN, since it is the medium that best reflects the characteristics of the materials. In this context, M7 was selected due its high IF (≈2) and high Q (≈ 10.5 μmol g^{-1}). M9 is also a promising material due to its Q value of 14 μmol g^{-1}. Jointly with the MIPs, the non-imprinted

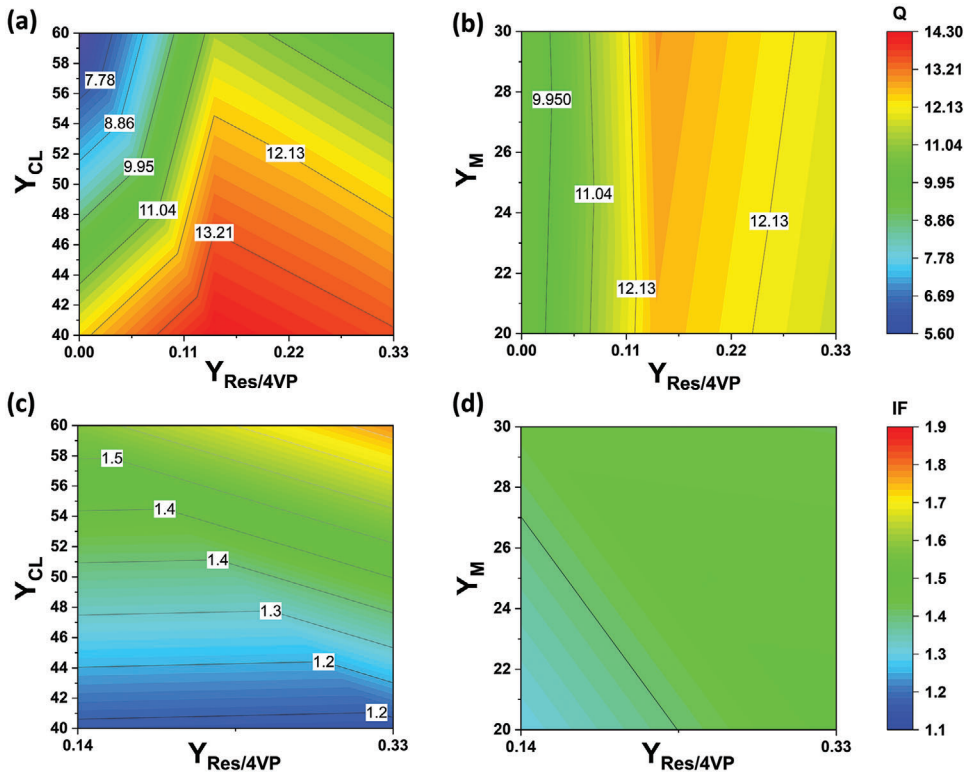

Figure 6. a,b) Contour plots of the combined effects of the crosslinker content (Y_{CL}), total monomer concentration (Y_M) and resveratrol content ($Y_{Res/4VP}$) on *Q*. c,d) Contour plots of the combined effects of the crosslinker content (Y_{CL}), total monomer concentration (Y_M) and resveratrol content ($Y_{Res/4VP}$) on IF.

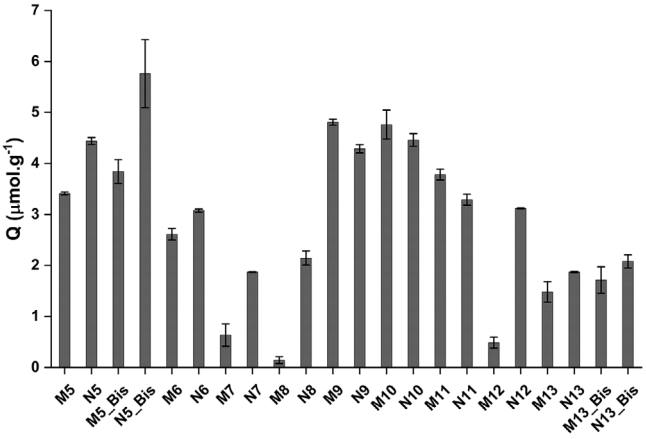

Figure 7. Binding capacity of the synthesized materials using 0.1 × 10^{-3} M trans-resveratrol in EtOH–water (8:2) and at room temperature ($n = 2$).

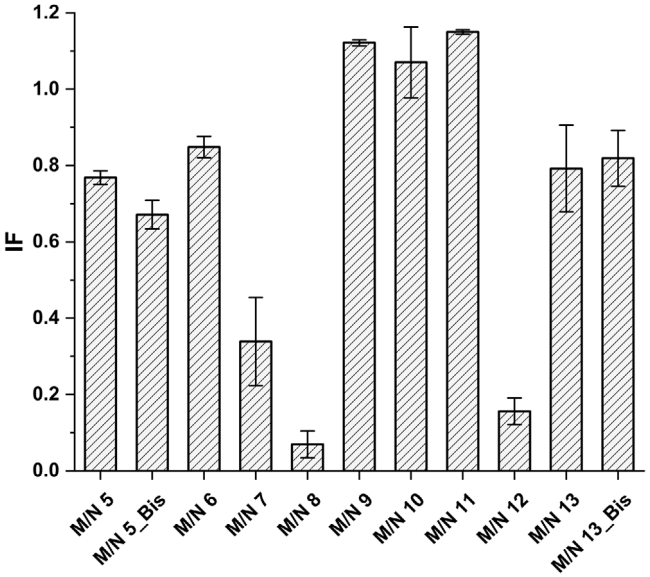

Figure 8. Imprinting factor (IF) of the synthesized materials using 0.1 × 10^{-3} M trans-resveratrol in EtOH–water (8:2) and at room temperature ($n = 2$).

polymers N7, N9 were also selected to treat the different extracts of grape stems. Although M13 had the highest IF of all the materials (≈3) with a reasonable binding capacity (8 µmol g^{-1}), its use in the SPE cartridge was not possible because of particle leakage, which is a direct consequence of a low Y_M (≈14%).

Obviously, before proceeding with the treatment of the grape extracts, trans-resveratrol was identified in both extracts of ACN and EtOH–water by injecting a trans-resveratrol standard. Information regarding this identification is annexed in Figure S6 (Supporting Information). Moreover, the calibration curve of trans-resveratrol is shown in Figure S7 (Supporting Information) and the parameters of the equation are listed in Table S8 (Supporting Information).

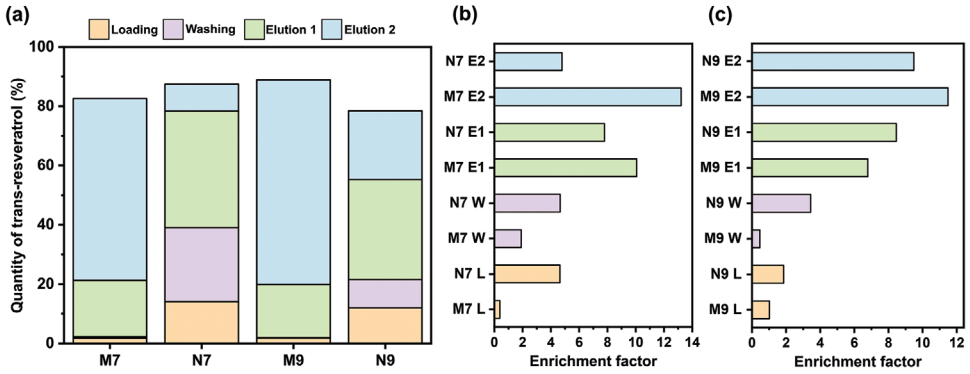

Figure 9. ACN grape stems extract treatment. a) SPE assessment of the synthesized materials (percentage of trans-resveratrol in each fraction is plotted). b) Enrichment factors of trans-resveratrol in each SPE fraction for the materials M7 and N7. c) Enrichment factors of trans-resveratrol in each SPE fraction for the materials M9 and N9. L refers to loading, W refers to washing, E1 refers to elution 1 and E2 refers to elution 2.

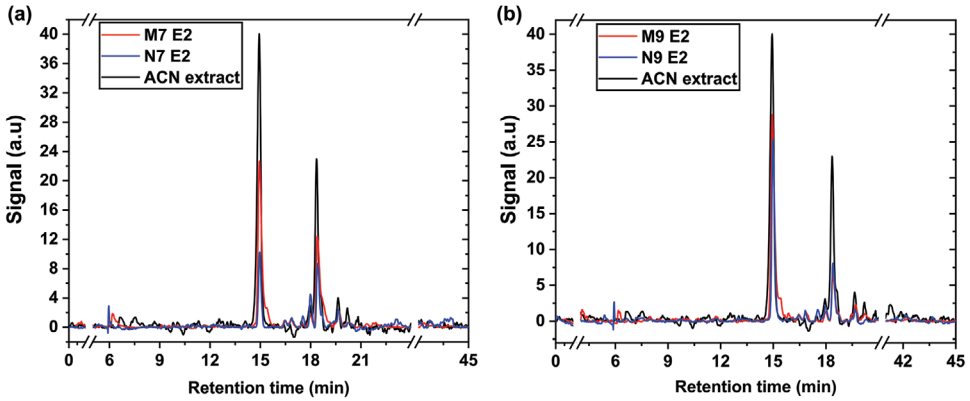

Figure 10. Chromatograms of the initial grape stems extract (in ACN) and the correspondent elutions of the materials M7, N7, M9 and N9 (measurement at $\lambda = 280$ nm).

5.2. Treatment of the ACN Extract

Solid phase extraction is a simple technique allowing the assessment of the binding capacity and selectivity of adsorbents vis-à-vis different analytes. The previously chosen materials (M7, N7, M9, and N9) were tested using this technique. For each material, four fractions were obtained which are the loading, washing, elution 1 (using EtOH–water 8:2) and elution 2 using (MeOH–AcOH 8:2). Using liquid chromatography, the quantity of trans-resveratrol was determined in each fraction. Consequently, the quantification of trans-resveratrol allowed the calculation of the enrichment factor in each fraction. The results are presented in **Figure 9**. A step-by-step analysis of the present results shows a clear difference between the molecularly imprinted materials (M7 and M9) and the corresponding non-imprinted ones (N7 and N9). The quantity of trans-resveratrol in the loading fractions of the MIPs is lower than the NIPs showing that the analyte was preferably retained from the ACN extract by the imprinted materials. Furthermore, the washing fractions (made also by ACN) show a higher quantity of trans-resveratrol in the NIPs than the MIPs which is expected since it is much harder to remove the retained trans-resveratrol from the 3D cavities of the MIPs than the polymeric networks of the NIPs. For the first elution (Elution 1), EtOH–water (8:2) was used to attempt the elution of the retained trans-resveratrol. This solvent was chosen because it is eco-friendly and sorption experiments in this medium showed a low retention of trans-resveratrol meaning that it should be easily eluted from the materials. The SPE assessment graph shows that the eluted quantity of trans-resveratrol is higher for the NIPs than the MIPs. Until this step, the recovery of trans-resveratrol from N7 and N9 was around 80% and 60% respectively while from M7 and M9 the recovery was around 20% for both materials. Thus, the use of another solvent to elute the remaining quantity of trans-resveratrol is necessary. Thus, in the last step (designated as elution 2), a mixture of MeOH–AcOH (8/2; v/v) was used. This allowed to further recover trans-resveratrol from the materials. The enrichment bars corresponding to elution 2 show an enrichment factor of almost 14 times for M7 and 12 times for M9. The chromatograms of elution 2 are shown in **Figure 10** and are compared with initial ACN extract of grape stems. Furthermore, **Figure 11** shows a 3D view of the ACN extract jointly with the fraction obtained using M9 (a similar 3D graph for M7 is annexed in Figure S8, Supporting Information). These results clearly show the advantage of using molecular imprinting technique as a tool to functionalize materials appropriate for continuous processes of fractionation or/and enrichment.

Regarding the peak appearing around 18 min in the ACN extract, an identification was attempted relying on the

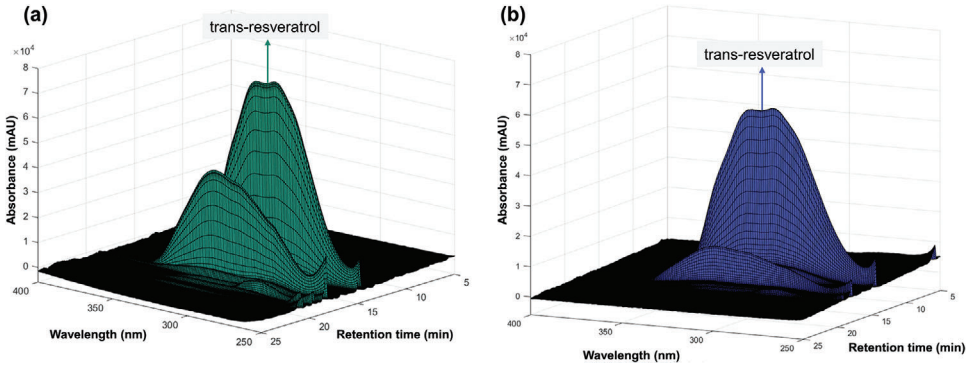

Figure 11. HPLC-DAD analysis of a) the ACN extract of grape stems and b) a fraction of this extract recovered in MeOH–AcOH (8:2) (elution 2) using the functionalized polymer M9.

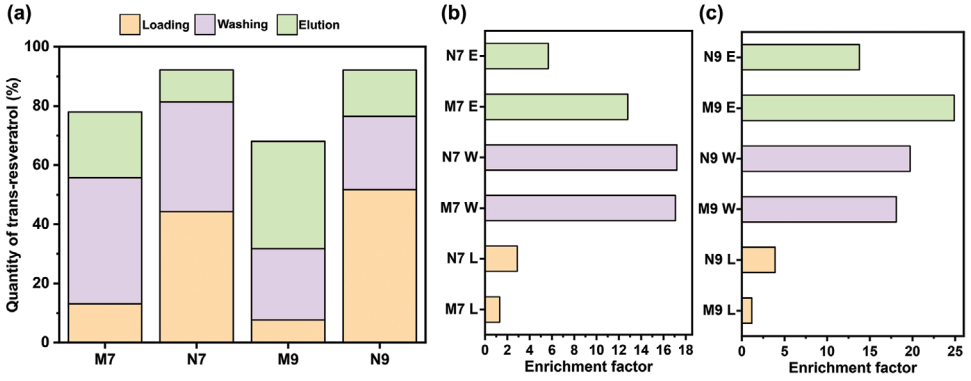

Figure 12. EtOH–water grape stems extract treatment. a) SPE assessment of the synthesized materials (percentage of trans-resveratrol in each fraction is plotted). b) Enrichment factors of trans-resveratrol in each SPE fraction for the materials M7 and N7. c) Enrichment factors of trans-resveratrol in each SPE fraction for the materials M9 and N9. L refers to loading, W refers to washing, E1 refers to elution 1 and E2 refers to elution 2.

chromatographic analysis as well as data found in literature. As shown in Figure S6 (Supporting Information), besides trans-resveratrol, another glycosylated stilbene was injected which is polydatin (also known as piceid). This latter elutes at around 10.5 min whereas trans-resveratrol elutes around 14.8 min. Thus, it is clear that the more hydroxyl groups the stilbene has, the earlier it will elute from the chromatographic column. Moreover, the UV spectrum of the compound at 18 min is close to the ones of trans-resveratrol and polydatin, which indicates that these compounds belong to the same family of phenolic compounds. To consolidate the proposed hypothesis, literature was consulted. According to Flamini et al., where the authors discuss the different stilbenes and their occurrence in grapes and derivative products (i.e., wine and winemaking residues), the compound eluting at 18 min is suggested to be of such kind (e.g., the presence in grape of pterostilbene (3,5-dimethoxy-4'-hydroxystilbene) or trans-resveratrol-4'-methyl ether is therein reported).[30]

5.3. Treatment of the EtOH W Extract

The same materials used to treat the previous ACN extract, were also used for the treatment of EtOH–water extract of grape stems and the SPE results are shown in **Figure 12**. Surprisingly, M7 and M9 appear to recognize trans-resveratrol in the hydroalcoholic mixture (both materials exert higher retention than N7 and N9). During the washing step, there is no significant difference between MIPs and NIPs which agrees with the sorption experiments carried out in the EtOH–water medium. However, in the elution step (MeOH–AcOH, 8/2 v/v), the imprinted materials are releasing more trans-resveratrol than the non-imprinted ones, confirming that the analyte was retained in the specific cavities of the MIPs, and using a strong protic solvent permits the liberation of these retained molecules. The chromatograms of the elutions are presented in **Figure 13** and 3D plots of the HPLC-DAD analysis regarding M7 and M9 elutions are attached in Figures S9–S11 (Supporting Information), respectively. Based on this experimental output, it can be asserted that the molecularly imprinted polymers are viable adsorbents for the enrichment of trans-resveratrol even when this latter is present in an interfering environment as the water ethanol mixture.

6. Conclusions

Functional polymer networks to target trans-resveratrol in winemaking residues were synthesized through UV irradiation at room temperature considering 4VP, styrene, and EGDMA as comonomers and AIBN as initiator. An approach based on the experimental design was considered for the selection of the

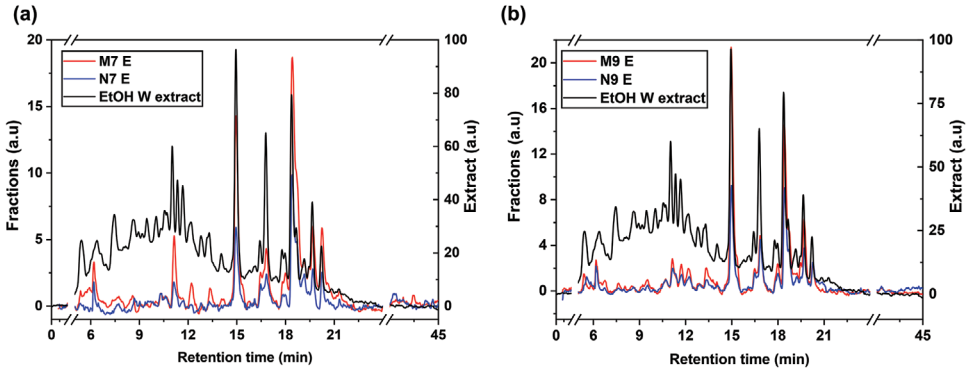

Figure 13. Chromatograms of the initial grape stems extract (in EtOH–W) and the corresponding elutions of the materials M7, N7, M9, and N9 (measurement at $\lambda = 280$ nm).

polymerization recipes leading to materials combining high retention capabilities and selectivity towards the target molecule when used as adsorbents. In this context, molecularly imprinted and non-imprinted polymers were both produced and assessed in sorption tests involving two solvents: pure ACN and EtOH–water (8:2).

The trans-resveratrol standard was used in these sorption tests which allowed the screening of parameters that impact the materials' performance. Factors like the crosslinker content (Y_{CL}) and the ratio of 4VP to trans-resveratrol ($Y_{Res/4VP}$) were found to strongly impact the molecular recognition of the materials as well as their binding capacity to trans-resveratrol. As a matter a fact, the results have demonstrated that using trans-resveratrol in the polymerization mixture improves substantially the imprinting factors as well as the adsorptive capacities of the materials which evidence the benefit of the molecular imprinting technique. Nevertheless, the yield of the polymerizations is negatively affected by the addition of trans-resveratrol in the polymerization mixture which is an anticipated outcome due to the antioxidant activity of this bioactive compound. It has been also shown that the type of solvent used in the sorption tests influences the materials' performances. For example, a strongly protic solvent (compared to ACN) like a hydroalcoholic mixture, would disturb the hydrogen bonding between the trans-resveratrol and the 4VP-based material, causing a decrease in both the binding capacity and the selectivity of a material.

Among the 30 synthesized, four promising materials (two pairs of MIP-NIP polymer networks) were selected for the enrichment of trans-resveratrol in grape stem extracts (ACN and EtOH–water solvents were considered). We show that enrichment factors of up to 12 folds were possible when using these materials as adsorbents in sorption/desorption processes. These results evidence the benefits of polymer functionalization through molecular imprinting in real sample processing (i.e., grape stems extracts).

Further optimization of the polymerization recipes using the outputs of this study (e.g., contour plots, linear models), large-scale production of functionalized polymers and enhancement of the sorption/desorption processes (e.g., the definition of solvent composition gradients) are future tasks to be addressed in the framework of the circular bioeconomy devoted to the efficient valorization of winemaking residues.

Supporting Information

Supporting Information is available from the Wiley Online Library or from the author.

Acknowledgements

The authors are thankful for the financial aid provided by "BacchusTech-Integrated Approach for the Valorization of Winemaking Residues" (POCI-01-0247-FEDER-069583), supported by the Competitiveness and Internationalization Operational Program (COMPETE 2020), under the PORTUGAL 2020 Partnership Agreement, through the European Regional Development Fund (ERDF). The authors are also grateful to the national funding by the Foundation for Science and Technology (FCT, Portugal) through the PhD grant of UI/BD/153688/2022.

Conflict of Interest

The authors declare no conflict of interest.

Data Availability Statement

The data that support the findings of this study are available from the corresponding author upon reasonable request.

Keywords

molecularly imprinted polymers, photopolymerization, polymer functionalization, trans-resveratrol enrichment, valorization of winemaking residues

Received: December 9, 2022
Revised: January 3, 2023
Published online: January 18, 2023

[1] E. Blasco, M. B. Sims, A. S. Goldmann, B. S. Sumerlin, C. Barner-Kowollik, *Macromolecules* **2017**, *50*, 5215.
[2] X. Chen, T. Michinobu, *Macromol. Chem. Phys.* **2022**, *223*, 2100370.
[3] J. J. Belbruno, *Chem. Rev.* **2019**, *119*, 94.
[4] H. Yan, K. Row, *Int. J. Mol. Sci.* **2006**, *7*, 155.

[5] S. Pardeshi, S. K. Singh, *RSC Adv.* **2016**, *6*, 23525.
[6] R. Zhang, R. Gao, Q. Gou, J. Lai, X. Li, *Polymers* **2022**, *14*, 1851.
[7] Y. Suzuki, R. Mishima, A. Matsumoto, *Int. J. Chem. Kinet.* **2022**, *54*, 361.
[8] Y. Lu, C. Li, X. Wang, P. Sun, X. Xing, *J. Chromatogr.* **2004**, *804*, 53.
[9] N. Corrigan, J. Yeow, P. Judzewitsch, J. Xu, C. Boyer, *Angew. Chem., Int. Ed.* **2019**, *58*, 5170.
[10] M. Worzakowska, *Polymers l* **2021**, *13*, 1659.
[11] S. H. Siyal, M. Li, H. Li, J.-L. Lan, Y. Yu, X. Yang, *Appl. Surf. Sci.* **2019**, *494*, 1119.
[12] H. Lai, X. Peng, L. Li, D. Zhu, P. Xiao, *Prog. Polym. Sci.* **2022**, *128*, 101529.
[13] M. Fabjanowicz, J. Płotka-Wasylka, J. Namieśnik, *TrAC, Trends Anal. Chem.* **2018**, *103*, 21.
[14] X. Meng, J. Zhou, C.-N. Zhao, R.-Y. Gan, H.-B. Li, *Foods* **2020**, *9*, 340.
[15] J. Tomé-Carneiro, M. Larrosa, A. González-Sarrías, F. Tomás-Barberán, M. García-Conesa, J. Espín, *Curr. Pharm. Des.* **2013**,*19*, 6064.
[16] M. Ji, Q. Li, H. Ji, H. Lou, *Food Chem.* **2014**, *142*, 61.
[17] S. Kurita, T. Kashiwagi, T. Ebisu, T. Shimamura, H. Ukeda, *Biosci. Biotechnol. Biochem.* **2014**, *78*, 499.
[18] D. P. Makris, G. Boskou, N. K. Andrikopoulos, P. Kefalas, *Eur. Food Res. Technol.* **2008**, *226*, 1075.
[19] B. Sun, A. M. Ribes, M. C. Leandro, A. P. Belchior, M. I. Spranger, *Anal. Chim. Acta* **2006**, *563*, 382.
[20] B. Dirion, Z. Cobb, E. Schillinger, L. I. Andersson, B. Sellergren, *J. Am. Chem. Soc.* **2003**, *125*, 15101.
[21] A. Bzainia, R. C. S. Dias, M. R. P. F. N. Costa, *Molecules* **2022**, *27*, 6406.
[22] C. P. Gomes, R. C. S. Dias, M. R. P. F. N. Costa, *Chromatographia* **2019**, *82*, 893.
[23] V. Khaimov, T. Reske, C. Matschegewski, N. Grabow, T. Eickner, *Curr. Dir. Biomed. Eng.* **2019**, *5*, 331.
[24] F. Navarro-Villoslada, B. S. Vicente, M.aríá C. Moreno-Bondi, *Anal. Chim. Acta* **2004**, *504*, 149.
[25] J. Cao, C. Shen, X. Wang, Y. Zhu, S. Bao, X. Wu, Y. Fu, *Carbohydr. Polym.* **2021**, *251*, 117026.
[26] C. P. Gomes, R. C. S. Dias, M. R. P. F. N. Costa, *React. Funct. Polym.* **2021**, *164*, 104930.
[27] C. P. Gomes, V. Franco, R. C. S. Dias, M. R. P. F. N. Costa, *Chromatographia* **2020**, *83*, 1539.
[28] C. Gomes, G. Sadoyan, R. Dias, M. Costa, *Processes* **2017**, *5*, 72.
[29] L. J. Schwarz, B. Danylec, S. J. Harris, R. I. Boysen, M. T. W. Hearn, *J. Chromatogr A* **2011**, *1218*, 2189.
[30] R. Flamini, F. Mattivi, M. Rosso, P. Arapitsas, L. Bavaresco, *Int. J. Mol. Sci.* **2013**, *14*, 19651.